Energy Equip. Sys./ Vol. 7/No. 1/March 2019/ 41-56

ENERGY EQUIPSYS

Energy Equipment and Systems

http://energyequipsys.ut.ac.ir
www.energyequipsys.com

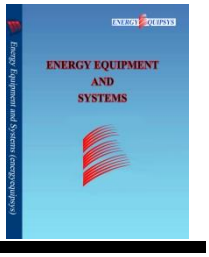

Modification of pump as turbine as a soft pressure reduction systems (SPRS) for utilization in municipal water network

Author

Hossein Yousefi [a],
Younes Noorollahi [a]
Mojtaba Tahani [a*]
Roshanak Fahimi [a]

[a] Faculty of New Sciences and Technologies, University of Tehran, Tehran, Iran

Article history:

Received : 7 July 2018
Accepted : 18 July 2018

ABSTRACT

Pressure Reducing Valves (PRV) are being used for decreasing the existing extra pressure in the water distribution network. however, they dissipate a considerable amount of energy. Therefore, the idea of application of Soft Pressure Reducing Systems (SPRS) is proposed, where a PRV is replaced by a hydropower station. The heart of An SPRS is the turbo-generator. One of the advantages of this type of hydropower plants is the opportunity of application of reverse pumps as the turbine. The performance of PATs is very susceptible to the flow amount and geometrical parameters. Therefore, the performance optimization of PATs is essential. In this research study, the performance of a PAT is investigated using computational fluid dynamics and four geometrical modifications are applied in order to improve its performance. The investigated geometrical parameters are volute type and diameter, beveling the impeller blade tip, deviation of the blade inlet angle. Results indicated that the utilization of radial volutes would be suitable when the flow is less than its BEP value most of the time and tangential volutes are suitable for the opposite situation. Decreasing the diameter would increase both the produced power and the efficiency but its influence is more significant for flows less than BEP. moreover, the results indicate that at a forward deviation equal to 5 degrees, the optimum performance of the turbine will be achieved.

Keywords: Pump as Turbine; Geometrical Modification; Hydropower Plant; CFD.

1. Introduction

Energy and water are the common problems of all countries around the world [1-3]. According to the energy crisis, increasing air pollution and greenhouse gases, governments are paying more attention to the renewable energies, efficiency of the power plants and also energy recovery systems. In several research studies [4-6], it can be seen that small hydropower plants have played an important role in the development of several countries especially rural areas. Small hydropower plants can be developed over rivers runoffs, channels or in water networks. According to the span of water distribution networks and also the topography of the area, the pressure of the water increases. Therefore, the utilization of pressure reduction valves (PRV) is essential to the purpose of creating pressure balance in the network and also preventing the network from damages. A significant amount of energy is being dissipated by the explained technology, so nowadays, it is recommended to use soft pressure reduction systems (SPRS) in which the valve is replaced by a hydro turbine. Water distribution networks provide excellent opportunities for harnessing the existing

[*] Corresponding author: Mojtaba Tahani
Faculty of New Sciences and Technologies, University of Tehran, Tehran, Iran
Email: m.tahani@ut.ac.ir

renewable energy in water flow. This energy provides both environmental and economic advantages. One of the economic advantages of this type of hydropower plants is their hydro turbine type. Reverse pumps or pumps as turbines (PAT) can be used as the mechanical converter and therefore they reduce the initial costs of the power plant. PATs performance is strongly influenced by flow variation. So after selecting the suitable PAT, a detail performance investigation is required using computational fluid dynamics (CFD). CFD is one of the most reliable tools in investigating the detail performance of pumps [7-9].

1.1.Literature Survey

Several research studies have been conducted in the field of investigating PAT performance. Chapallaz et al. [10] developed a manual for the utilization of pumps as turbines and tried to develop empirical equations according to the performance curves of PATs. Singh [11] investigated the performance of the PAT experimentally at different velocities and increased the performance of the PAT using different geometrical corrections. Derakhshan and Nourbakhsh [12,13] carried out research studies in the field of numerical, theoretical and empirical performance of PAT and they developed equations for estimating the performance of the PAT. Also, their research study indicated that beveling of the leading edge of the blade, hub ,and shroud increases the efficiency of the PAT. Singh and Nestmann [14] developed new equations for PAT selection and also predicting its performance and their results indicated that an error equal to 10 to 30% exists between experiment and theory. Yang et al. [15] studied the influence of volute geometry on the pump performance at a specific speed equal to 23, using ANSYS-CFX software by implementing $RNG\ k-\varepsilon$ turbulence model. Their investigations indicated that a volute with a circle cross section has higher efficiency in comparison to rectangular and trapezoidal sections. Nautiyal et al. [16] empirically investigated the performance of the pump and developed new relations for predicting the PAT performance. The results indicated that these equations are acceptable for specific speeds between 20 to 40. Fecarotta et al. [17] numerically estimated the PAT performance. The influence of reducing the elements size and also the type of flow were investigated and the results indicated that for achieving more accurate results, the element size must be as small as possible and also the effects of transient flow have significant effects on performance prediction. Dribssa et al. [18] investigated the performance of a reverse pump using numerical methods at different flow rates. The results indicated that at the best efficiency point, the numerical results are in a good agreement with experimental data. Li [19] investigated the flow of stable fluids with different viscosities in both pump and turbine mode, using numerical and empirical methods. tTheir results indicated that by increasing viscosity, the flow velocity, total head, and hydraulic efficiency will increase at the best efficiency point. Jafarzadeh et al. [20] studied the characteristics of a 3D flow in a PAT using the $k-\varepsilon$ model. They investigated the influence of the number of the blades on the pump efficiency and they evaluated the important factors which affect the flow separation. Guo et al. [21], investigated the interactions between the impeller and the casing of a centrifugal pump using the SST turbulence model and CFX software. Zhou et al. [22] indicated that the best turbulence model for simulating the performance of a PAT is the SST model. Rodrigues et al. [23], investigated the performance of a number of pumps in turbine mode using numerical simulations and compared the results with experimental data. They showed that the efficiency of the PAT is almost the same as the pump mode. Hongjuan et al. [24] investigated experimentally the effect of pressure fluctuations in a pump turbine. Williams [25] conducted a research study in the field of a pump as turbines performance prediction methods. Eight methods were used for this purpose while the results indicated that none of them gives an accurate prediction. In the study conducted by Zeng et al. [26], a theoretical basis for predicting the characteristics curves of PATs has been provided. The transient characteristics and flow behaviors in the startup process of PAT has been investigated by Li et al. [27] in three dimensional numerical simulation. Fernandez et al. [28] evaluated the functional characterization of a centrifugal pump used as a turbine. The results indicated that the turbine characteristics can be predicted to some extent from the pump characteristics.

The aim of this research study is to investigate the influence of geometrical parameters of a PAT, which is going to be used as a hydro turbine for an SPRS. Four geometrical parameters namely:

- The volute casing type
- The volute diameter

- Impeller blade beveling
- Deviation of blade inlet angle

Are investigated using CFD calculations. The utilized method first has been validated using experimental data and after that, the best geometrical configuration of the PAT at different operational conditions has been illustrated using the numerical method. The main novelty of the presented study can be summarized in the application type of the PAT and also the involvement of its most critical geometrical parameters in the study at different operational conditions.

1.2.Reverse pump selection

Several researchers have developed theoretical equations for selecting a suitable reverse pump for a specific operating condition. However, there is no general equation for this purpose and each of these equations can be utilized for pumps with specific hydraulic and geometrical characteristics. Figure 1 illustrates the operational range of different types of PAT.
In order to select a suitable PAT, the flowchart presented in Fig.2 must be applied.

According to Fig.2, the final step of the PAT selection procedure is CFD analysis. It amplifies the importance of numerical simulation in The PAT selection process. In this research study, first the governing equations are presented, and then the discretization procedure with the suitable turbulence model are explained. After that, numerical simulations of a pump, in both pump and turbine modes are provided. The results of the simulations are provided and are discussed in section (3).

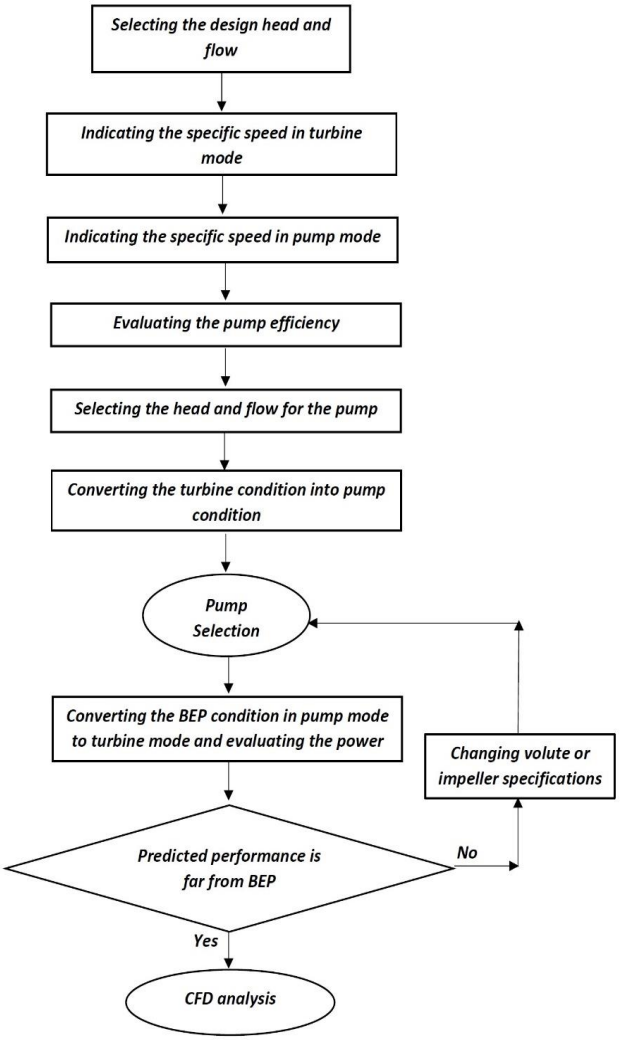

Fig 1. PAT selection flowchart

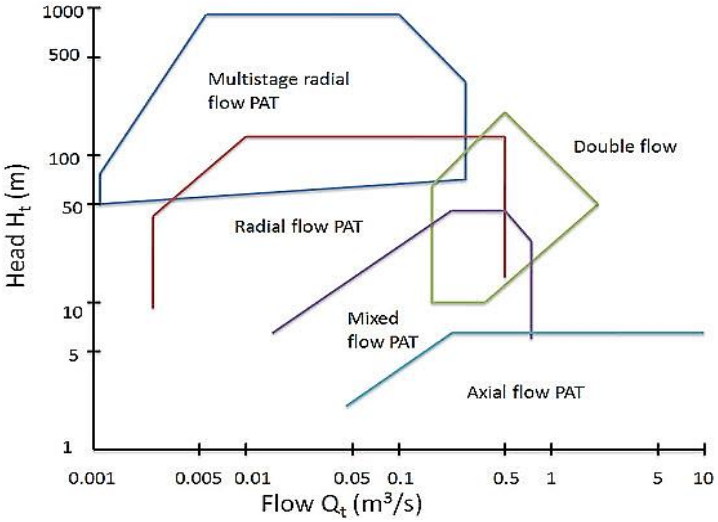

Fig 2. The operational condition of different types of PATs

Nomenclature

Q	flow rate (m^3/h)
P	power (kW)
H	head (m)
S	source term
B_2	passage width of Impeller (mm)
BEP	best efficiency point
CFD	computational fluid dynamics
SST	The shear stress transport model
n	impeller rotating speed, (r/min)
PAT	pump as a turbine
u	peripheral velocity, (m/s)

Greek symbols

ρ	density (kg/m^3)
β_1	outlet angle of the blade(degree)
β_2	outlet angle of blade(degree)
τ	average shear stress on the wet wall (Pa)
η	efficiency (%)
Ω	rotational speed (rpm)
ω	rotational angular speed of impeller (rad/s)
μ	dynamic viscosity of liquid (Pa.s)

Subscripts

I,j	components

2. Numerical method

In this research study, Ansys CFX software has been utilized for the purpose of solving the three dimensional Reynolds-averaged Navier-Stokes equations at different working conditions. In this software, the equations are discretized and solved based on control volume and finite element interpolation method with saved values at computational nodes. The Implicit technique is utilized and there are no restrictions for time intervals; therefore the number of iterations would decrease and the convergence would occur faster [29]. Utilization of Ansys CFX software, especially in turbomachinery and aerodynamic flows, will cause fast and precise results. Also, it has the capability of processing different parts of turbomachines before and after simulations and the post-processing can be easily achieved. For the purpose of discretization in the space axis, a higher-order method is implemented.

2.1.Governing Equations

The main governing equations in the simulation of the flow characteristics are the continuity and momentum transfer equations. Because in a reverse pump, the fluid in the impeller is rotated around an axis, the governing equations must be written in two domains. These two are rotating and stationary domains. For this reason, the multi-reference frame (MRF) method is used for expressing the equations. In governing equations, the centrifugal and also Coriolis forces are expressed as source terms. According to the incompressibility of the fluid and also steady flow, the continuity equation can be expressed as follow:

$$\frac{\partial U_i}{\partial x_j} = 0 \tag{1}$$

The momentum conservation equation can be expressed as follow by adding the source and averaged shear stress terms:

$$\frac{\partial(\rho\overline{u_\iota u_J})}{\partial x_i} = -\frac{\partial \bar{P}}{\partial x_i} + \frac{\partial\left[\bar{\tau}_{ij} - \rho\overline{u'_\iota u'_J}\right]}{\partial x} - S_{ui} \tag{2}$$

In the above equation, the velocity components are expressed as relative velocities. The source term ,as mentioned earlier, contains the centrifugal and Coriolis forces and can be expressed as Eq.(3). In this equation, the gravity effects are neglected, and this is for the reason that the height difference between the inlet and outlet is so small.

$$S_{ui} = -\rho\left[2\vec{\Omega} \times \vec{u} + \vec{\Omega} \times \left(\vec{\Omega} \times \vec{r}\right)\right] \tag{3}$$

$$\bar{\tau}_{ij} = -\mu\left(\frac{\partial \bar{u}_i}{\partial x_j} + \frac{\partial \bar{u}_j}{\partial x_i}\right) \tag{4}$$

In the above equations, ρ and υ are the density and kinematic viscosity of the fluid respectively and Ω and x are presenting the rotational speed of the relative coordinate and position vector respectively.

For the purpose of solving a turbulent flow, the properties of the flow are being divided into two components, a time-averaged and fluctuating, and all equations are getting averaged in time. by averaging the momentum equation, the turbulent terms, $\overline{u_\iota u_J}$ are achieved, which are called Reynolds stresses.

$$\tau_{ij} = -\rho\,\overline{u_\iota' u_J'} = \mu_T\left(\frac{\partial \overline{u_\iota'}}{\partial x_j} + \frac{\partial \overline{u_J'}}{\partial x_i}\right) - \frac{2}{3}\left(\rho k + \mu_T \frac{\partial u_k}{\partial x_k}\right)\delta_{ij} \tag{5}$$

These equations cannot be solved because of the appearance of turbulent terms. Therefore, usually, the Reynolds stresses are approximated by velocity gradients using turbulence models.

2.2.Turbulence Model

Turbulence models are used for simplicity and also including the effect of fluctuations in all directions. Several turbulent models are proposed based on Reynolds averaged Navier Stokes equations so far. But a general model which can be used for all kind of flow regimes and applications has not been developed.

The most applicable turbulence models are two equation models which are based on the relation between the turbulent viscosity with length scale and fluctuated velocity. In these models, a balance exists between the computational cost and the accuracy. Epsilon based turbulence models predict the separation so late and also less than its real value. Therefore $k-\omega$ models are developed for solving this problem.

In the general $k-\omega$ models, the turbulent frequency (ω) is being utilized instead of destruction rate (ε). $k-\omega$ equations were developed by Wilcox for low Reynolds numbers [30]. The transfer equations for k and ω are as follow:.

$$\frac{\partial}{\partial t}(\rho k)+\frac{\partial}{\partial x_i}(\rho k u_i)= P-\beta^*\rho\omega k+\frac{\partial}{\partial x_i}\left[(\mu+\sigma_k\mu_t)\frac{\partial k}{\partial x_i}\right] \tag{6}$$

$$\frac{\partial}{\partial t}(\rho\omega)+\frac{\partial}{\partial x_i}(\rho\omega u_i)= \frac{\gamma\omega}{k}P-\beta\rho\omega^2+\frac{\partial}{\partial x_i}\left[(\mu+\sigma_\omega\mu_t)\frac{\partial\omega}{\partial x_i}\right] \tag{7}$$

$$P=\tau_{ij}\left(\frac{\partial u_i}{\partial x_j}\right) \tag{8}$$

$$\mu_T=\frac{\rho k}{\omega} \tag{9}$$

Among $k-\omega$ models, the shear stress transport $k-\omega$ (SST $k-\omega$) model has been developed for predicting the time and also amount of separation accurately in presence of inverse pressure gradient. The SST $k-\omega$ model has been developed by Menter by combining the standard $k-\omega$ approach for near wall region and standard $k-\varepsilon$ approach for free stream region far from the wall. In another words, the model has the capabilities of both $k-\omega$ and $k-\varepsilon$ models.

For the purpose of investigating the flow characteristics in a centrifugal pump, the SST turbulence model has been utilized [31]. In order to transfer the turbulent shear stress, the vorticity viscosity is calculated using the following equation where S is the shear rate.

$$\mu_T=\frac{\rho k}{\omega}\frac{1}{max\left[\frac{1}{\alpha^*},\frac{SF_2}{a_1\omega}\right]} \tag{10}$$

In Eq. (10), S, F_2 and α^* are calculated separately.

2.3.Equations discretization and solving method

The numerical method which is used in this study utilizes a hybrid method for discretizing the fluid domain into a finite number of control volumes and then it uses the finite element method in contact with the geometry. The numerical procedure which is used in this study contains a finite number of meshes which is illustrated in Fig.3. All variables and also fluid properties are saved in each node.

Mass and momentum conservation equations in Cartesian coordinate are integrated for each control volume and the Gaussian divergence theorem is used for converting all volume integrals to surface integrals. The final equations can be written as follow:

$$\frac{\partial}{\partial t}\int_v\rho dv+\int_s\rho u_j dn_j=0 \tag{11}$$

$$\frac{\partial}{\partial t}\int_v\rho u_i dv+\int_s\rho u_j u_i dn_j= -\int_s P dn_i+\int_s\mu\left(\frac{\partial u_i}{\partial x_j}+\frac{\partial u_j}{\partial x_i}\right)dn_j+\int_s S_{u_i}dv \tag{12}$$

$$\frac{\partial}{\partial t}\int_v\rho u_i\varphi dv+\int_s\rho u_j\varphi dn_j= -\int_s\Gamma\left(\frac{\partial\varphi}{\partial x_j}\right)dn_j+\int_s\mu\left(\frac{\partial u_i}{\partial x_j}+\frac{\partial u_j}{\partial x_i}\right)dn_j+\int_v S_\varphi dv \tag{13}$$

where V and S are presenting the volume integral and surface integral respectively, and dn_j is the Cartesian derivative component of surface normal vector. Volume integrals are presenting source terms while surface integrals

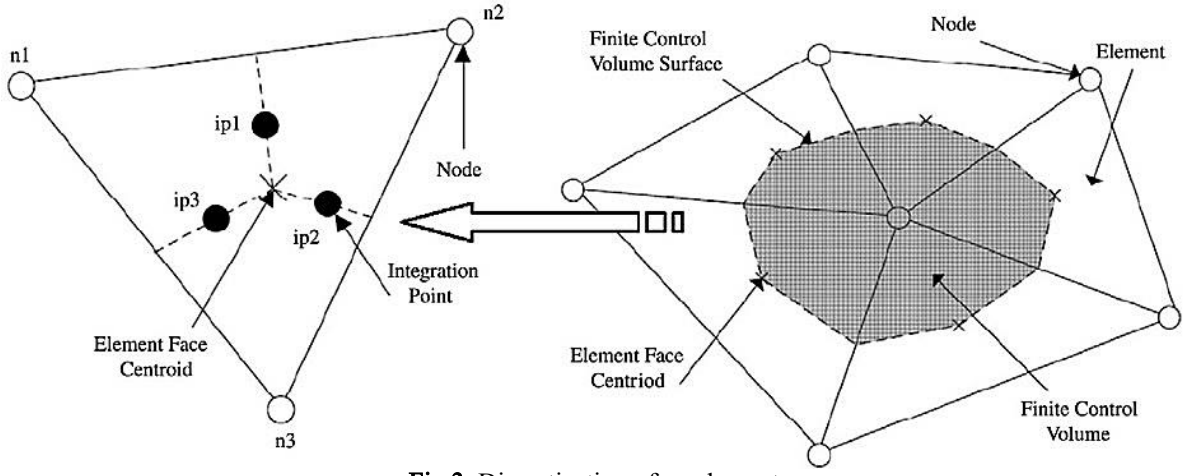

Fig.3. Discretization of an element

are representing the sum of flows. The next step in the numerical algorithm is discretization of volume and surface integrals. After discretization of volume and surface integrals, the integral equations can be rewritten as follow:

$$\rho V\left(\frac{\rho-\rho^{\circ}}{dt}\right)+\sum_{ip}\left(\rho u_i dn_j\right)_{ip}=0 \tag{14}$$

$$\rho V\left(\frac{u_i-u_i^{\circ}}{dt}\right)+\sum_{ip}\dot{m}_{ip}(u_i)_{ip}= \sum_{ip}\left(\rho dn_j\right)_{ip}+\sum_{ip}\left(\mu\left(\frac{\partial u_i}{\partial x_j}+\frac{\partial u_j}{\partial x_i}\right)dn_j\right)_{ip} + \overline{S_{u_i}}V \tag{15}$$

$$\rho V\left(\frac{\varphi-\varphi^{\circ}}{dt}\right)+\sum_{ip}\dot{m}_{ip}\varphi_{ip}= \sum_{ip}\left(\Gamma\left(\frac{\partial \varphi}{\partial x_j}\right)dn_j\right)_{ip}+ \sum_{ip}\left(\mu\left(\frac{\partial u_i}{\partial x_j}+\frac{\partial u_j}{\partial x_i}\right)dn_j\right)_{ip}+\overline{S_{\varphi}}V \tag{16}$$

In the above equations, $\dot{m}_{ip}$ equals to $\left(\rho u_j \Delta n_j\right)_{ip}^{\circ}$, V presents the control volume, dt is the time step, dn_j is the discretized surface normal vector, subscript ip represents an integral point and superscript ° is the previous time step and also the sum of all integral points series of control volume.

2.4.Boundary Condition

For the reverse pump, the inlet and outlet boundary conditions are set as the total pressure and mass flow rate respectively. For the stationary and rotary walls with a relative roughness equal to 100 μm, no-slip condition is applied. water is set as working fluid with density equal to 998 kg/m^3 and a kinematic viscosity equal to 1×10^{-6} m^2/s in 25°C. because the flow is considered to be developed the turbulence intensity is set equal to 5%. at both outlet and inlet. In Table (1), all boundary conditions for different parts of the reverse pump is tabulated.

Table 1. Selected boundary conditions

Domain Name	Domain Motion	Surfaces	Boundary Condition
Volute	Stationary	Volute Casing Wall	Smooth no Slip Wall
		Volute Casing Inlet	Frozen Rotor Interface
		Volute Casing Outlet	Inlet
Impeller	Rotating	Impeller Hub	Smooth no Slip Wall
		Impeller Shroud	Smooth no Slip Wall
		Impeller Blade	Smooth no Slip Wall
		Impeller Inlet	Outlet
		Impeller Outlet	Frozen Rotor Interface

3.Results and Discussions

For the purpose of numerical simulation, first, the three-dimensional model of the impeller and volute must be developed. The specification of the selected pump impeller and volute are tabulated in Table (2) and their three-dimensional models are developed using CFturbo software, which is presented in Fig. (4) and Fig. (5).

Table 2. Specification of different parts of selected pump

Part	Specification	Value
Impeller	Number of blades	6
	Suction diameter	116
	Impeller diameter	259
	Outlet width	19
	Blade angle β_1	28.9
	Blade angle β_2	36.7
	Blade thickness shroud	3
	Blade thickness hub	5
Volute	Volute type	Single volute
	Inlet width	32
	Inlet diameter	286
	Design rule	215
	Diffuser height	280
	Outlet	100

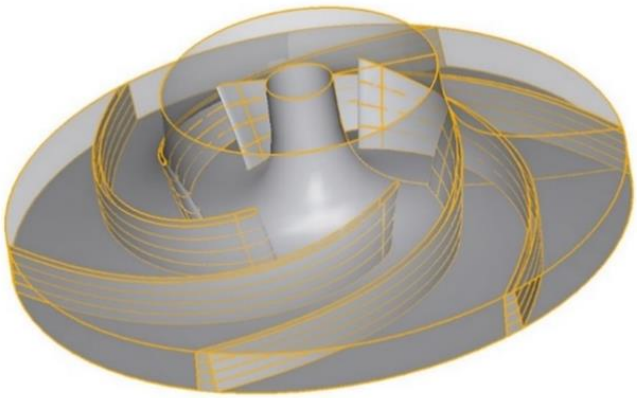

Fig 3. The designed impeller using CFturbo software

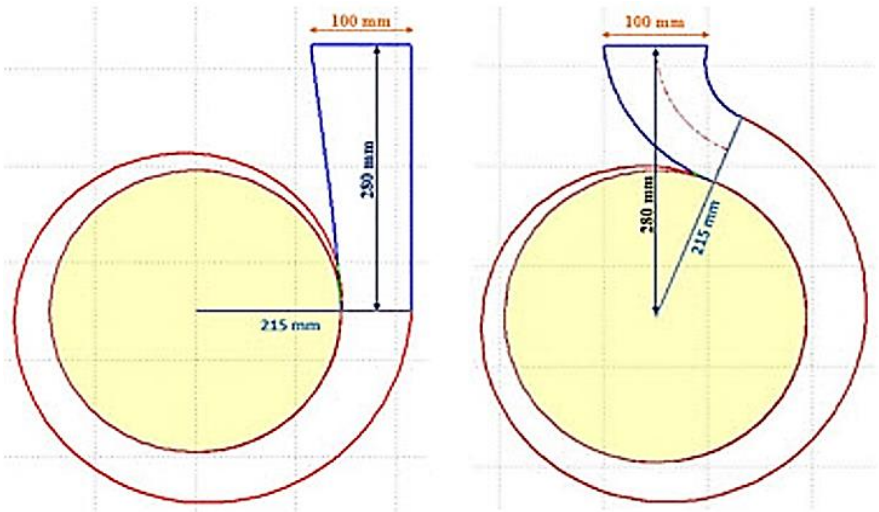

Fig 4. Radial and tangential volutes designed by CFturbo

For grid generation, ANSYS ICEM CFD software is utilized. This software has the capability of creating structured and unstructured meshes. The geometry of the pump has been divided into two parts for the purpose of grid generation. In order to decrease the number of elements and also achieve a suitable answer, a combination of tetragonal and hexagonal elements has been utilized. In Fig.6 the generated grid for the tangential and radial volutes is illustrated.

On the impeller, 1324733 elements are utilized with the average values of orthogonality and elongation equal to 0.85634 and 0.27636 respectively \. The values of orthogonality and elongation for tangential volute are equal to 0.84412 and 0.26419 respectively and for radial volute, these values are 0.84838 and 0.27141, which indicates the great quality of the mesh. In Table (3), a summary of mesh statistics is presented.

In order to check for a mesh independent solution, the outlet pressure and the impeller torque were selected as the evaluation parameters. According to Fig7, the number of elements for the selected mesh is equal to 2844016.

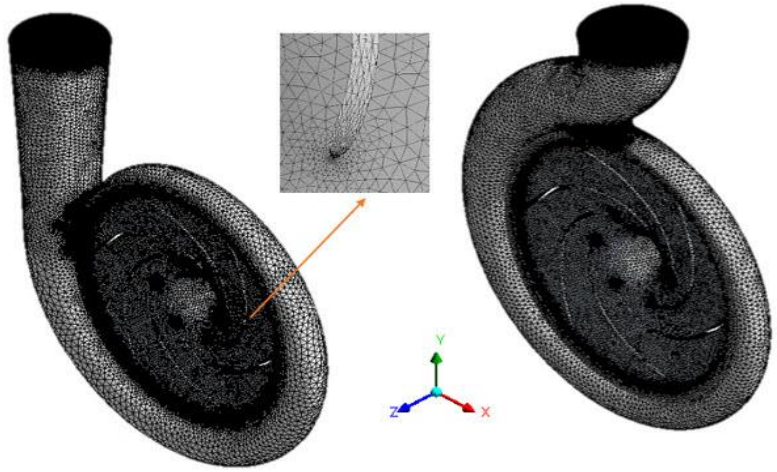

Fig 5. Generated grid for radial and tangential volutes

Table 3. A summary of mesh statistics

Component	Number of Nodes	Number of Elements
Impeller	461873	1324733
Radial Volute Casing	541853	1627642
Tangential Volute Casing	535807	1519283

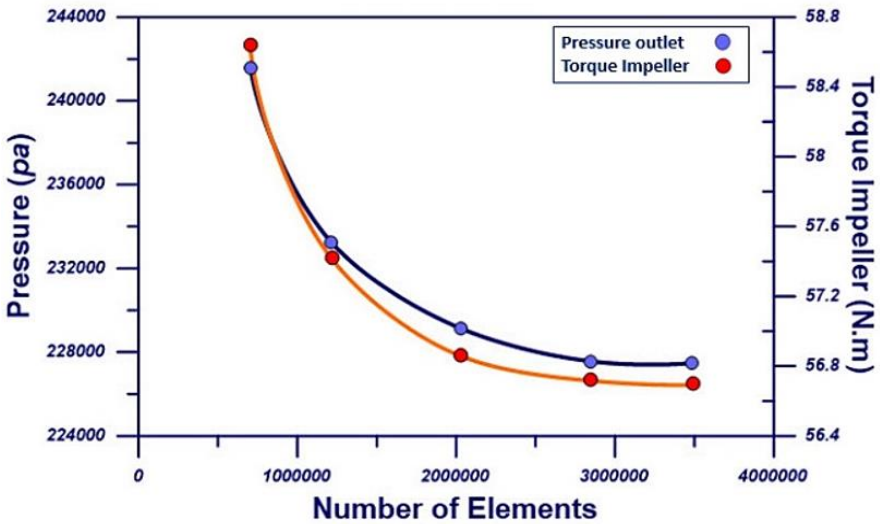

Fig 6. Mesh independency study

3.1.The pump simulation results

In this research study, the numerical analysis of the centrifugal pump has been carried out in five flow rates: 60, 90, 120, 150 and 180 m^3/h at a rotational speed equal to 1450 rpm. For each of these flow rates, the pressure distribution at the midplane and the outlet head amount has been calculated. The numerical results are compared with existing empirical results of 100-250 Pump Iran pump [32], with a diameter equal to 259mm and the results are in agreement with each other. The values of the head, efficiency, and power of the pump are calculated using the following equations:

$$Head = \frac{P_{Total\ Out} - P_{Total\ In}}{\gamma} \quad (17)$$

$$Power = T_{All\ Blades} \times \omega \quad (18)$$

$$Efficiency = \frac{\gamma \times Q \times Head}{Power} \quad (19)$$

In Table (4), the numerical and experimental values of pump efficiency, head, and power are illustrated. The average error for those parameters is 5.14%, 2.62%, and 8.32% respectively. Figure 8 illustrates the pressure contours at the pump midplane at different flows.

3.2.Reverse pump simulation results

For the purpose of investigating the PAT performance empirically, an experimental setup was developed which is illustrated in Fig.9. According to this figure, water is pumped using a submersible pump. First, it passes through a pressure sensor and pressure reducing valve for the purpose of regulating pressure on the required value. After that, it passes through a flow meter and it enters into the PAT. At the outlet, a second pressure reducing valve is positioned which creates the in pipe discharge situations. The produced power has been evaluated at inlet pressure equal to 60 m and flow rates equal to 120,150,180 and 220 m^3/h.

The values of the head, power, and efficiency in the case of PAT are calculated using the following equations:

$$Head = \frac{P_{Total\ In} - P_{Total\ Out}}{\gamma} \quad (20)$$

$$Power = T_{All\ Blades} \times \omega \quad (21)$$

$$Efficiency = \frac{Power}{\gamma \times Q \times Head} \quad (22)$$

According to the presented pressure contours in Fig.10, increasing the flow values causes an increase of pressure in the volute and impeller and also the rotational speed of the impeller. The difference between the numerical and experimental results of PAT is more significant in comparison to pump results. This is due to the reason that at turbine mode, the flow direction is reversed and at the inlet of blades, a significant amount of dissipation occurs. Table (5) illustrates the numerical and experimental results. The average error between experimental and numerical results of efficiency, head, and power of PAT is 4.64%, 6.14%, and 14.5% respectively, which are acceptable.

Table 4. A comparison between numerical and empirical values of head, power, and efficiency of 100-250 pump [24]

Flow rate (m^3/h)	Empirical head (m)	Numerical head (m)	Empirical power	Numerical power	Empirical efficiency (%)	Numerical efficiency (%)
60	22	21.09	5.5	4.986	65	69.01
90	21	20.57	6.8	6.309	76	79.8
120	19.2	18.69	7.9	7.293	81	83.62
150	16.7	16.14	8.8	8.096	78	81.31
180	12.8	12.919	9.5	8.61	69	73.86
Average error(%)	2.62		8.32		5.14	

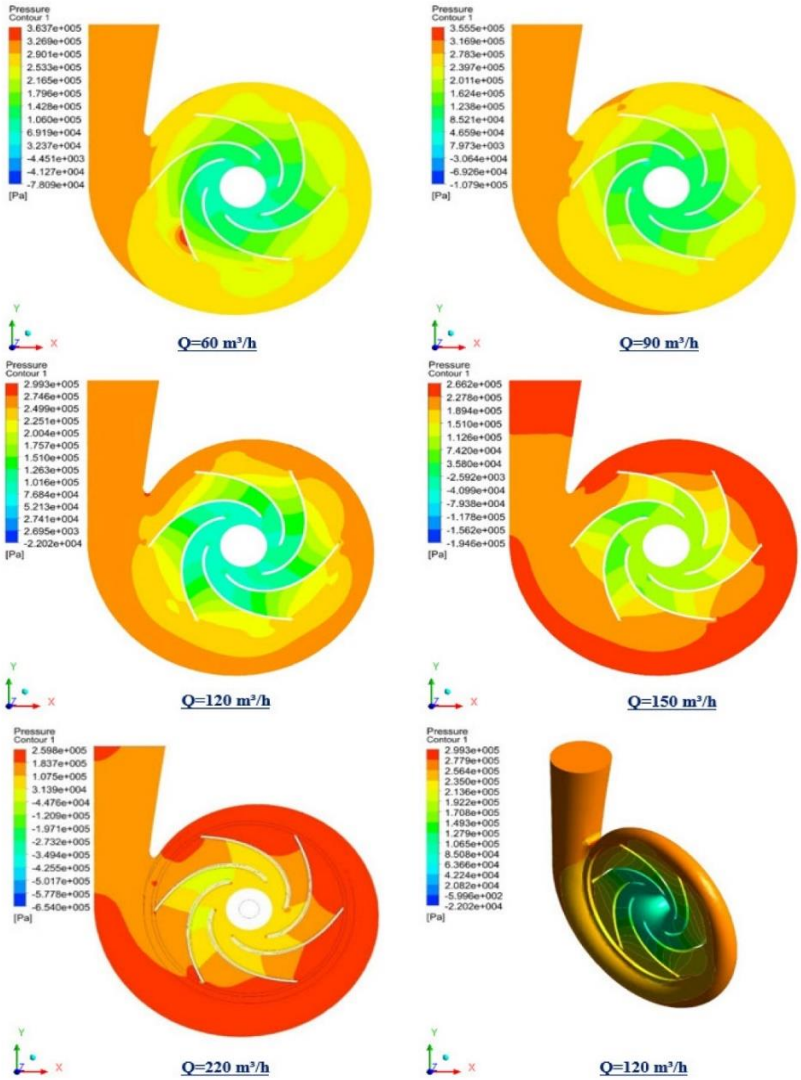

Fig 7. Pressure contours at the midplane of the pump

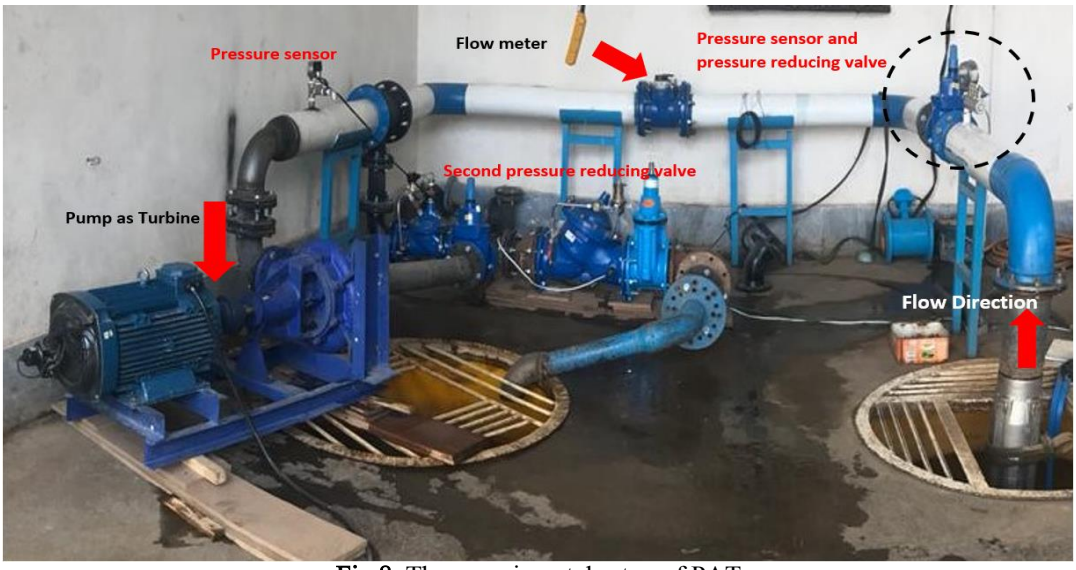

Fig 8. The experimental setup of PAT

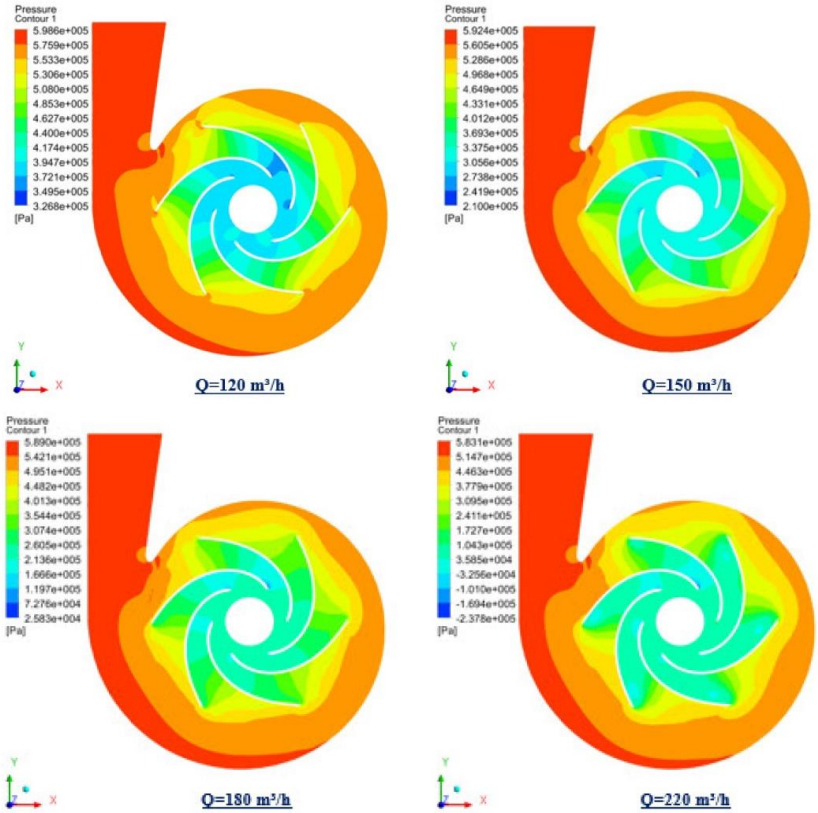

Fig 9. Pressure contours at the mid plane of PAT

Table 5. Numerical and experimental results of PAT

Flow rate (m^3/h)	Experimental head (m)	Numerical head (m)	Experimental power	Numerical power	Experimental efficiency	Numerical efficiency
120	21.13	22.31	4.05	4.996	65.25	68.62
150	25.88	27.19	7.61	8.376	72.08	75.52
180	29.36	30.41	10.82	11.650	75.28	78.26
220	32.7	36.08	12.65	14.783	64.65	67.54
Average error (%)	6.14		14.5		4.64	

3.3.Geometrical modifications for improving the PAT performance

3.3.1.Volute type

Two types of volutes were considered, namely radial casings and tangential casings. According to the investigation, different results can be achieved for turbine and pump modes and according to the flow rate value, the type of the volute can be selected.

According to the Fig.11 and Fig.12, at BEP condition and also at small flow rates, utilization of radial volutes can increase the head and torque with a percentage equal to 2.64% and 3.681% respectively in comparison to tangential volutes. at larger flow rates, utilization of tangential volutes will increase the head and torque with a percentage equal to 2.02% and 4.86% respectively in comparison to radial volutes. At BEP point, no significant difference exists between these two types of volutes but in general, the radial volute has better performance.

3.3.2.Volute diameter

Volute diameter is an important parameter, which affects the hydraulic performance of the PAT, . In this section, the influence of decreasing the volute diameter up to 5 mm has been investigated on the head, torque, power,

and efficiency at different flow rates and the results are illustrated in Table (6). The current modification increases the average head and torque up to 10.34% and 13.5% respectively.

According to Fig.13, decreasing the diameter increases the efficiency at almost all flows. The amount of increment for the points below the BEM point is more significant.

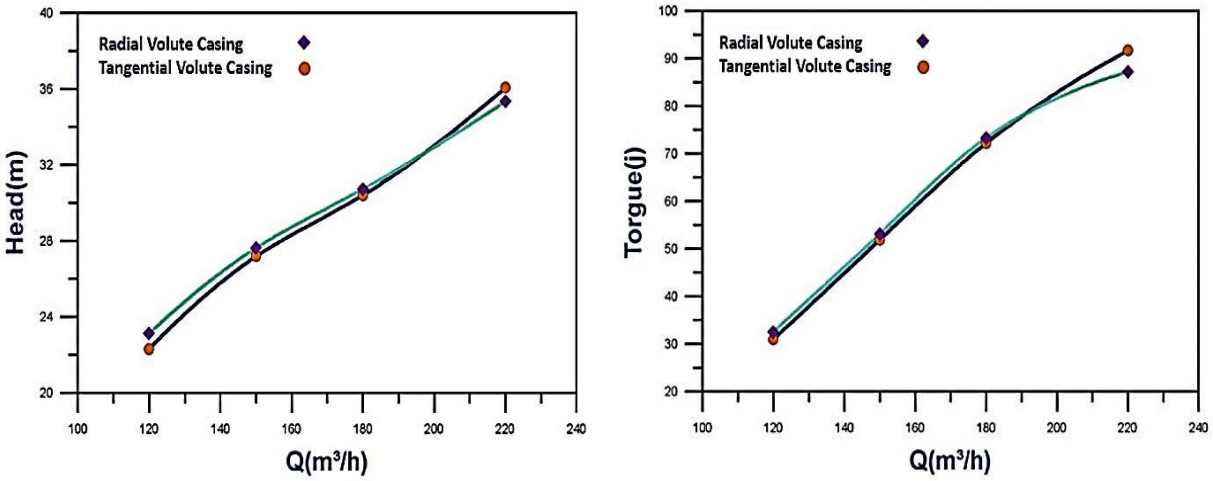

Fig 10. Head and torque variation of PAT for two different volutes

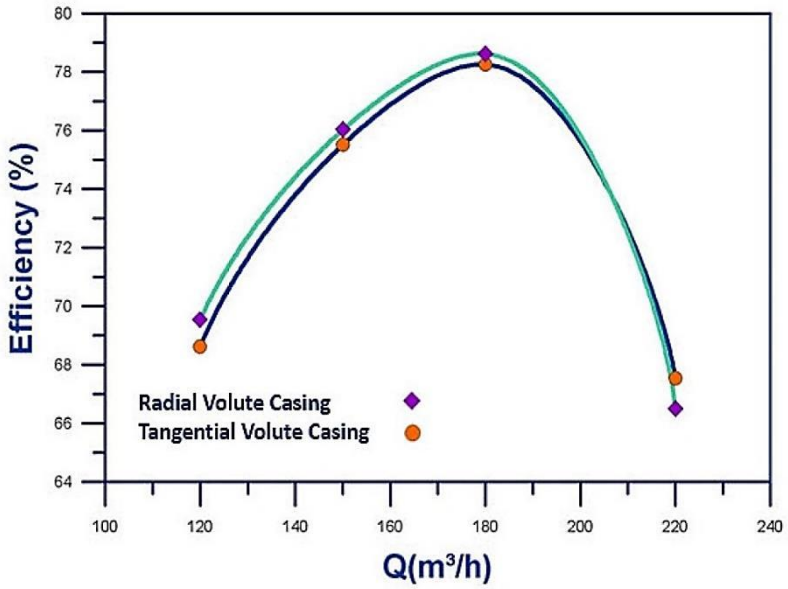

Fig 11. Variation of efficiency for two different volute casings at different flows

Table 6. Numerical values of head, power, and efficiency of original PAT and also modified PAT

Flow rate (m^3/h)	Original PAT head (m)	Modified PAT head (m)	Original PAT torque (N.m)	Modified PAT torque (N.m)	Original PAT power	Modified PAT power
120	22.31	23.41	30.98	33.86	4.996	5.461
150	27.19	29.87	51.94	58.93	8.376	9.503
180	30.41	34.25	72.24	83.67	11.650	13.493
220	36.08	41.12	91.67	105.79	14.783	17.060

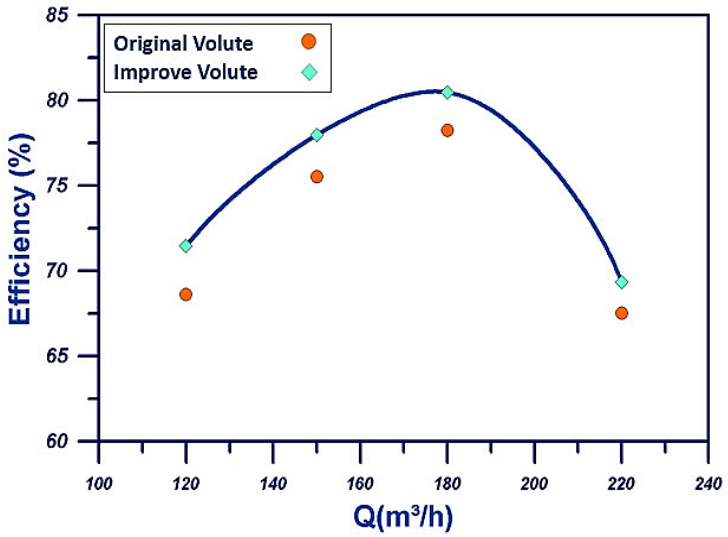

Fig 12. The variation of the original and modified PAT efficiency at different flows

3.3.3.Beveling the blade tips and changing the blades inlet angle

In order to increase efficiency, the tips of the blades are beveled and the influence of the amount of bevel has been investigated. Figure 14 shows the beveled blade. The radius of the bevel is half of the blade thickness. The numerical results indicated that efficiency could be increased by 1.2% in the beveled turbine.

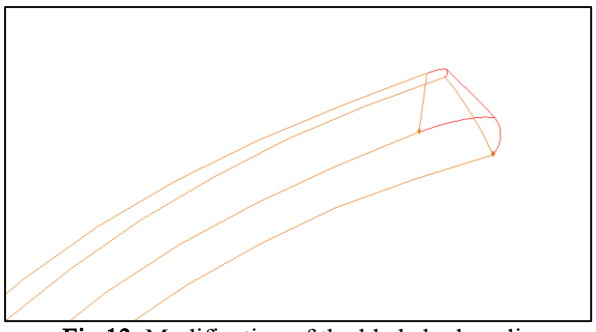

Fig 13. Modification of the blade by beveling

Contours of balanced static pressure, are one of the most important parameters which can be used for investigating the reason for increasing the efficiency of the beveled PAT. When the fluid is leaving the PAT, because of decreasing the hydraulic losses, the head is decreased in comparison to the initial state. In Fig.15 it can be seen that the pressure drop for a beveled pump is less than the conventional one.

For the purpose of investigating the influence of increasing and decreasing the blade inlet angle, forward and backward deviations are applied for this angle. The numerical results indicated that the pressure drop for backward angles is more than forward angles; therefore, a PAT with backward deviated blades has lower efficiency. In order to obtain the optimum angle, different forward deviation angles are analyzed and their efficiency is illustrated in Fig.16. The optimum deviation angle is equal to 5 degrees, which increases efficiency by 2%.

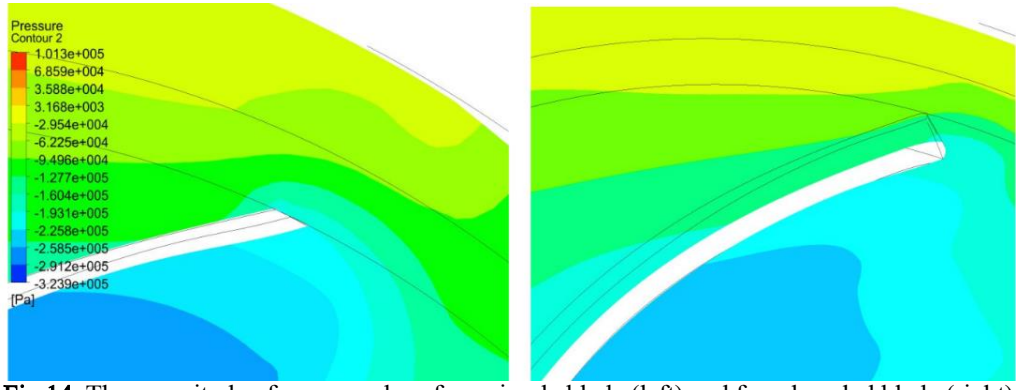

Fig 14. The magnitude of pressure drop for a simple blade (left) and for a beveled blade (right)

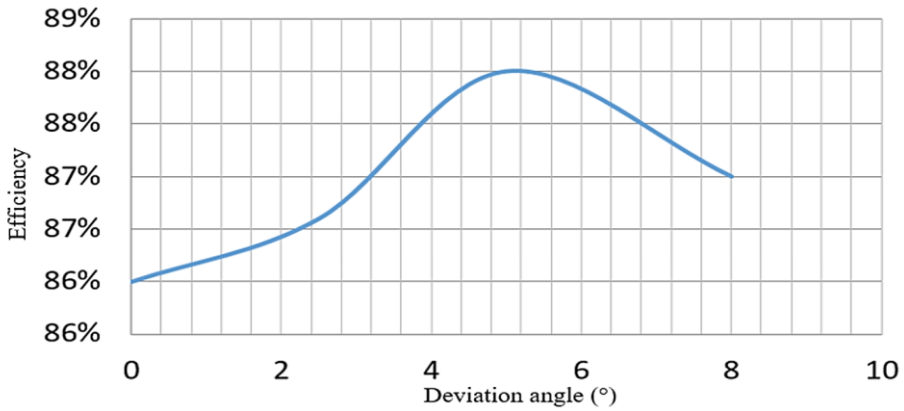

Fig 15. The PAT efficiency at different deviation angle

4.Conclusion

In this research study, it was aimed to investigate the performance of a pump as a turbine (PAT) using the CFD. The hydro turbine in an SPRS can be considered as the heart of the system. The importance of the investigated subject is in the vast application of PATs in micro hydropower plants and also the power plants which are being utilized in water distribution networks as the soft pressure reducing systems. Because of the topography of an area, at some points of the water network, the pressure increases and can causes damages. In order to prevent these damages, pressure reduction valves are being utilized. One of the disadvantages of this kind of valves is that they only reduce the pressure and therefore dissipate a lot of energy. These valves can be replaced by an SPRS in order to control the network pressure balance and also produce power. PATs are one of the best candidates for these applications. Therefore, in this research study, after validation of numerical method with experimental data of pump and also PAT, the following items were conducted and the results are summarized here:

- Four geometrical modifications were applied in order to investigate their influence on the PATs performance, which was: the influence of volute casing type, the influence of decreasing the volute diameter, the influence of beveling the blade tip and also the influence of the deviation of the blade inlet angle.
- The results indicated that the utilization of radial volutes is when most of the time, the flow is less than its BEP value and tangential volutes are suitable when the opposite occurs.
- The results also indicated that by decreasing the diameter, the produced power and also the efficiency would increase. This effect is more significant when the flow is less than BEP.
- The results also showed that at forward deviation equal to 5 degrees, the optimum performance of the turbine would be achieved.

References

[1] Ghaebi H., Bahadorinejad M., Saidi M.H., Energy Efficiency in a Building Complex through Seasonal Storage of Thermal Energy in a Confined Aquifer,The Journal of Energy Equipment and Systems, 5(4): 341-348(2017).

[2] Shahgholian G., Analysis and Simulation of Dynamic Performance for DFIG-Based Wind Farm Connected to a Distribution System. The Journal of Energy Equipment and Systems 6(2):117-130(2018).

[3] Derakhshan S., Moghimi M., Motawej H., Development of a Mathematical Model to Design an Offshore Wind and Wave Hybrid Energy System. The Journal of Energy Equipment and Systems 6(2):181-200 (2018).

[4] Ødegård H.L., Eidsvik J. & Fleten S,E., Value of Information Analysis of Snow Measurements for the Scheduling of Hydropower Production. The Journal of Energy Systems (2017). https://doi.org/10.1007/s12667-017-0267-3.

[5] Aasgård, E.K., Naversen, C.Ø., Fodstad, M. et al. : Optimizing day-ahead bid curves in hydropower production. The Journal of Energy Systems (2017).

https://doi.org/10.1007/s12667-017-0234-z.

[6] Alais J.C., Carpentier P., De Lara M., Multi-Usage Hydropower Single Dam Management: Chance-Constrained Optimization and Stochastic Viability. The Journal of Energy Systems (2017) 8: 7. https://doi.org/10.1007/s12667-015-0174-4.

[7] Weidong S., Ling Z., Weigang Bing L., Tao P. L., Numerical Prediction and Performance Experimental in a Deep-well Centrifugal Pump with Different Impeller Outlet Width. Chinese Journal of Mechanical Engineering, 26:46-52 (2013). https://doi.org/10.3901/CJME.2013.01.046

[8] Yi T., Shouqi Y., Jianrui L., Fan Z., Jianping T., Influence of Blade Thickness on Transient Flow Characteristics of Centrifugal Slurry Pump with Semi-open Impeller, Chinese Journal of Mechanical Engineering, 29: 1209-1217 (2016). https://doi.org/10.3901/CJME.2016.0824.098.

[9] Yuilang Z., Yi L., Baoling C., Zuchao Z., Huashu D., Numerical Simulation and Analysis of Solid-liquid Two-phase Flow in Centrifugal Pump, Chinese Journal of Mechanical Engineering, 26:53-60 (2013). https://doi.org/10.3901/CJME.2013.01.053

[10] Chapallaz J.M., Eichenberger P., Fischer G., Manual on Pumps used as Turbines, Vieweg Braunschweig, Germany (1992).

[11] Singh P., Optimization of the Internal Hydraulic and of System Design in umps as Turbines with Field Implementation and Evaluation, Ph.D. thesis, University of Karlsruhe, Karlsruhe (2005).

[12] Derakhshan S., Nourbakhsh A., Theoretical, Numerical and Experimental Investigation of Centrifugal Pumps in Reverse Operation, Experimental Thermal and Fluid Science, 32, 1620-1627 (2008). https://doi.org/10.1016/j.expthermflusci.2008.05.004.

[13] Derakhshan S., Nourbakhsh A., Mohammadi B., Efficiency Improvement of Centrifugal Reverse Pumps, Journal of Fluids Engineering, 131:1620-1627 (2009). doi:10.1115/1.3059700.

[14] Singh P., Nestmann F., Experimental Optimization of a Free Vortex Propeller Runner for Microhydro Application, Experimental Thermal and Fluid Science, 33:991-1002 (2009). https://doi.org/10.1016/j.expthermflusci.2009.04.007.

[15] Yang S., Kong F., Chen B., Research on Pump Volute Design Method Using CFD, International Journal of Rotating Machinery, 124 (2011). http://dx.doi.org/10.1155/2011/137860.

[16] Nautiyal H., Varun Kumar A., Yadav S., Experimental Investigation of Centrifugal Pump Working as Turbine for Small Hydropower Systems, Energy Science and technology, 1:79-86 (2011). doi:10.1088/1755-1315/16/1/012064.

[17] Fecarotta O., Carravetta A., Ramos H. M., CFD and Comparisons for a Pump as Turbine Mesh Reliability and Performance Concerns, International Journal of Energy and Environment, 2:39-48 (2011).

[18] Dribssa E., Nigussie T., Tsegaye B., Performance Analysis of Centrifugal Pump Operating as Turbine for Identified Micro/Pico Hydro Site of Ethiopia, International Journal of Engineering Research and general Science, 3:6-19 (2015).

[19] Guang Li, W., Effects of Viscosity on Turbine Mode Performance and Flow of a Low Specific Speed Centrifugal Pump, Applied Mathematical Modelling, 40, 904-926 (2016). https://doi.org/10.1016/j.apm.2015.06.015.

[20] Jafarzadeh B., Hajari A. , Alishahi M.M., Akbari M.H., The Flow Simulation of a Low Specific Speed High Speed Centrifugal Pump, Forschung Imingenieurwesen, 74:123-133 (2010). https://doi.org/10.1016/j.apm.2010.05.021.

[21] Guo P., Luo X., Lu J. , Zheng X., Numerical Investigation on Impeller-Volute Interaction in the Centrifugal Pump with Radial GAP and Tongue Profile Variation, In Fluid Machinery and Fluid Mechanics, Beijing, China (2009).

[22] Zhou P.J. , Wang F.J. , Yang M., Internal Flow Numerical Simulation of Double-Suction Centrifugal Pump Using DES Model, IOP Conference Series: Earth and Environmental Science, Beijing, China (2012).

[23] Rodrigues A., Williams A.A., Singh P., Nestmann F., LAI E., Hydraulic Analysis of a Pump as Turbine with CFD and Experimental Data, IMechE seminar, Computational Fluid Dynamics for Fluid Machinery, London, UK (2003).

[24] Hongjuan R. , Xianwu L. , Lei Z. , Yao Z., Xin W., Hongyuan X., Experimental Study of the Pressure Fluctuations in a Pump Turbine at Large Partial Flow Conditions, Chinese Journal of Mechanical Engineering, 25: 1205-1209 (2012). https://doi.org/10.3901/CJME.2012.06.1205.

[25] Williams A.A., The Turbine Performance of Centrifugal Pumps: A Comparison of Prediction Methods, Proceedings of the Institution of Mechanical Engineers, Part A: Journal of Power and Energy, 208:59-66 (1994).

[26] Zeng W., Yang J.D., Cheng Y.G. et al., Formulae for the Intersecting Curves of Pump-Turbine Characteristic Curves with Coordinate Plans in Three-Dimensional Parameter Space, Proceedings of the Institution of Mechanical Engineers, Part A: Journal of Power and Energy, 229: 324-336 (2015).

[27] Li Z., Bi H., Wang Z. et al., Three-Dimensional Simulation of Unsteady Flows in a Pump-Turbine During Start-up Transient up to Speed no-load Condition in Generating Mode, Proceedings of the Institution of Mechanical Engineers, Part A: Journal of Power and Energy, 230:570-585 (2016).

[28] Fernandez J., Bianco E., Parrondo J. et al., Performance of a Centrifugal Pump Running in Inverse Mode, Proceedings of the Institution of Mechanical Engineers, Part A: Journal of Power and Energy, 218: 265-271 (2004).

[29] Help Navigator, Ansys CFX, Release 12.0 CFX-Solver modeling Guide.

[30] Barbareli S., Amelio M. , Florio G., Predictive Model Estimating the Performances of Centrifugal Pump used as Turbines. Energy, 103:103-121 (2016). https://doi.org/10.1016/j.energy.2016.03.122.

[31] Alemi H., Nourbakhsh A. , Raisee M. , Najafi F., Effect of Volute Curvature on Performance of Low Specific-Speed Centrifugal Pump at Design and Off-Design Conditions, Journal of Turbomachinery, 137 (2015). doi: 10.1115/1.4028766.

[32] http://www.pumpiran.org/english/